

Influence of Order in Solutions of Polyvinylcarbanilate on Light Scattering Measurements

WALTHER BURCHARD

In solutions of polyvinylcarbanilates in diethyl ketone, methyl ethyl ketone and in acetone the Zimm plots show unusual inflections at low angles. These inflections are interpreted by external interferences. They arise from a certain order within the solutions, whereby the phases of scattered rays, belonging to different molecules, keep relative definite relationships. Quantitatively the measurements are evaluated by a formula due to Fournet, which was derived from a well known relationship of Zernicke and Prins. According to Fournet a repulsion potential between the macromolecules is effective and prevents the overlapping of segment clouds.

Two possibilities for the explanation of the repulsion potential are discussed. The one consists in the facility of intramolecular hydrogen bonds, which will fix the coil like wire netting, and the other possibility in strong solvation, whereby the solvent molecules become adsorbed within the coil. Furthermore it is shown that the intrinsic viscosities need up to three hours to reach a constant value if the temperature is suddenly changed. From this relaxation process an energy of activation of about 12 kcal per mole macromolecule is calculated.

TODAY, scattering of monochromatic visible light by high polymer solutions is one of the most common and reliable methods of determining the magnitude and shape of large particles. This method is applicable first, if the difference between the refractive indices of solvent and polymer is sufficiently high, because only then a scattering intensity due to the polymer is detectable, and secondly, if the diameter of the molecule is greater than a tenth of the light wavelength used. If both conditions are realized, the internal interferences can appear and are determined both by shape and magnitude of the scattering particles. These internal interferences manifest in typical angular distributions, the so-called shape factors $P(\vartheta)$ of the scattered light.

The shape factor is a relatively complicated function of the scattering angle ϑ , but for random coils of linear polymers straight lines are obtained to good approximation if $c/R(\vartheta)$ is plotted against $\sin^2 \vartheta/2$, where c is the concentration and $R(\vartheta)$ the absolute scattering intensity of the light.

Because of the interaction between the particles, $c/R(\vartheta)$ is dependent on the concentration and follows the equation

$$\frac{K \cdot c}{R(\vartheta)} = \frac{1}{M_w P(\vartheta)} + A_2 c \cdot Q(\vartheta) + \dots \quad (1)$$

where K is the optical constant, M_w the molecular weight, A_2 the second virial coefficient, and $P(\vartheta)$ and $Q(\vartheta)$ are shape factors.

As usual the light scattering measurements are evaluated from Zimm plots in which $Kc/R(\vartheta)$ is plotted against $\sin^2 \vartheta/2 + kc$, where k is an

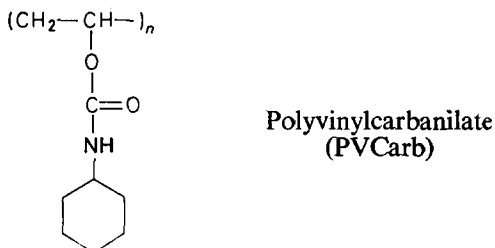
arbitrary constant¹. The slope of the extrapolated straight line at $c=0$ is given by

$$\text{slope} = \frac{16\pi^3 \langle S^2 \rangle}{3 \lambda^3 M_w} \quad (2)$$

where λ is the wavelength of the light in the solution and $\langle S^2 \rangle$ the mean square radius of gyration of the coil.

In general, linear non-electrolyte polymers yield Zimm plots with a group of approximately parallel straight lines. Only in a few cases are deviations, tending to smaller $c/R(\vartheta)$ values, observed at low angles. These are caused by the presence of a small number of very large particles like microgels, aggregates, or sometimes bacteria in aqueous solutions^{2,4}.

The solution properties of polyvinylcarbanilate (PVCarb) have been investigated⁵. In the most used solvents this polymer also yields normal



Zimm plots without any trouble. However, in diethyl ketone (DEK) unusual deviations are obtained, the interpretation of which is due neither to the presence of large particles nor to optical anisotropic molecules, like isotactic polystyrene, the effect of which has been discussed by Utiyama and Kurata^{6,7}.

EXPERIMENTAL

Polymer

Polyvinylcarbanilates are prepared by treating polyvinyl alcohol with phenyl isocyanate in pyridine at 100°C. The reaction is complete in two hours, the formerly heterogeneous mixture becoming a clear solution as the reaction takes place. Then the polymers are precipitated in methanol, washed several times, and reprecipitated from a dioxan solution in water. The polyvinyl alcohol is obtained by saponification of polyvinyl acetate, which was previously radically polymerized at room temperature. More details are published elsewhere⁸.

For the measurements a sharp middle fraction is chosen. The sample has a molecular weight of $M_w = 1.1 \times 10^6$ and a heterogeneity of $M_w/M_n = 1.1$, determined by fractionation of this fraction.

Light scattering

The light scattering measurements were performed with a Sofica photogoniometer using vertically polarized light. The angular distributions were measured partly in intervals of 15° both with the green and the blue Hg wavelength, and partly in intervals of 5° with the blue wavelength only. The measurements at the green wavelength were transformed to the measure-

ments at the blue wavelength. For this purpose the $\sin^2\theta/2$ values were multiplied by the factor $(436/546)^2$.

The solutions were purified by centrifugation for about one hour at 30 000 g in a Spinco ultracentrifuge model L.

Since the effect reported here is very sensitive to traces of moisture, special cells have been developed that can be closed to the humidity of the atmosphere. They consist of special optical glass and are fitted with a Teflon stopper. Such cells are available from Glastechnische Werke Hellma, Müllheim, Germany.

Solvents

Diethyl ketone from the Fluka Company, Buchs, Switzerland, was used. The water content of about 0.5 per cent was removed by drying with molecular sieves. Methyl ethyl ketone and acetone p.a. were products of Merck, Darmstadt, Germany.

Viscosity

The viscosity measurements were performed with Ostwald viscometers. First the solutions were put in a thermostat for about two hours; then the viscometers were put in another thermostat, the temperature of which was 10 deg. C above that of the first one. Measurements were started immediately. After two minutes the solvent had a constant value.

RESULTS

The results of light scattering measurements in diethyl ketone (DEK) at different temperatures are shown in *Figure 1*. At high temperatures normal Zimm plots are obtained; only at the highest concentration does a small inflection at low angles appear, but this lies within the experimental errors. However, these inflections become more pronounced with decreasing temperature and are detectable even at low concentrations. At lower temperatures the effect is very powerful making the evaluation of Zimm plots difficult and even impossible.

The same effect is observed in solutions of methyl ethyl ketone (MEK) and of acetone, although not to this extent. It is remarkable that the effect vanishes if precipitants like water or some alcohols are added to the solutions in MEK and acetone. Simultaneously a clear coil expansion takes place. This transition from one coil conformation to the other has been described elsewhere in detail⁵.

Another indication of an uncommon property of PVCarb in DEK is given by viscosity measurements. Usually a distinct state of the coil rapidly attains thermodynamic equilibrium when the temperature is changed, e.g. if a solution is put into a thermostat, a constant viscosity is obtained some minutes later. However, the solutions of PVCarb in DEK take up to three hours to attain constant viscosities, after the temperature has suddenly been raised. This behaviour is seen in *Figure 2*.

A QUALITATIVE INTERPRETATION

In Zimm plots the reciprocal scattering intensity is used. In this form it is difficult to find an idea for an explanation of the observed inflections. A

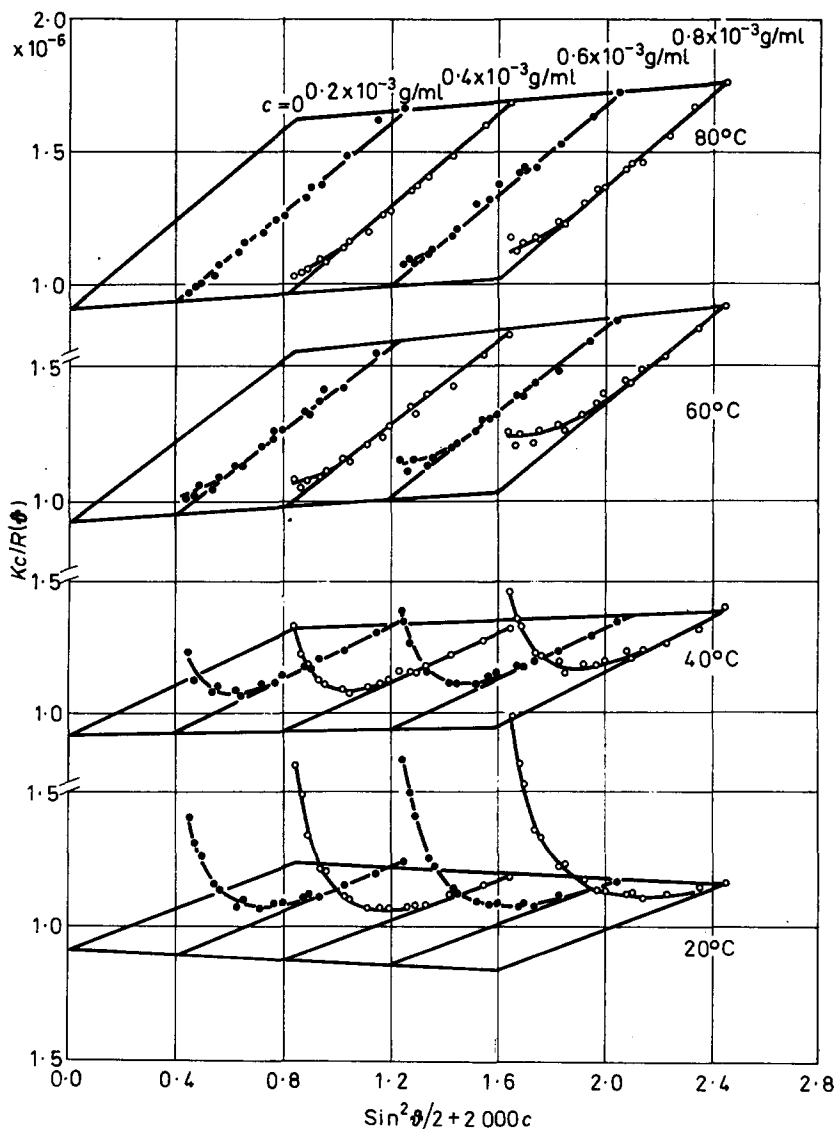


Figure 1—Zimm plots of polyvinylcarbanilate, $M_w = 1.1 \times 10^6$, in DEK at 80°, 60° 40° and 20° C. $\lambda = 4360 \text{ \AA}$

much better survey is obtained if the apparent shape factor, that is $P'(\vartheta) = R(\vartheta) M_w / Kc$, is plotted against the scattering angle ϑ . For example, at 50°C the curves of Figure 3 are obtained. The broken line corresponds to the extrapolated straight line in the Zimm plot. At high angles all curves coincide with the dotted line, which might be considered as the unperturbed shape factor $P(\vartheta)$. At low angles the scattering intensity is strongly reduced, the more so the larger the concentration.

INFLUENCE OF ORDER OF SOLUTIONS OF POLYVINYL CARBANILATE

The same effect, which is very uncommon in light scattering, has been known for many years in the field of X-ray small angle scattering. There the deviations from the true shape factor have been interpreted by external

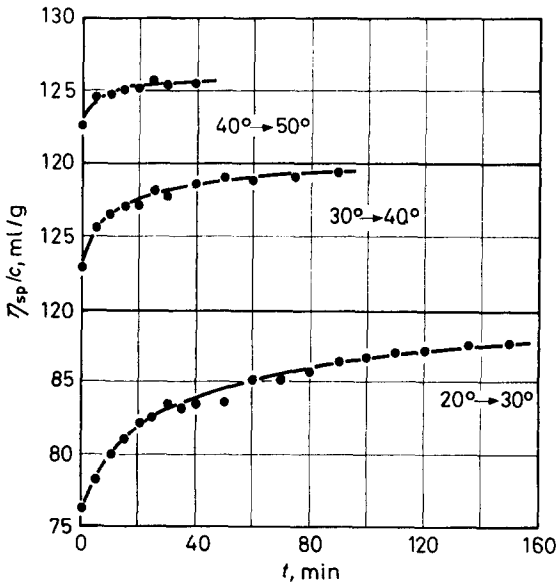


Figure 2—Dependence of η_{sp}/c on time after a sudden 10 deg. C change in solution temperature. The symbol $20^\circ \rightarrow 30^\circ$ means the temperature change from 20° to 30° C. Concentration of polymer is $c = 4.56$ g/l.

interferences, which are caused by interparticle scattering^{9,16}. The interparticle scattering is dependent on the order within the system, because the relationships of phases between the scattered waves of different molecules become more definite when the molecules are better ordered in space. An

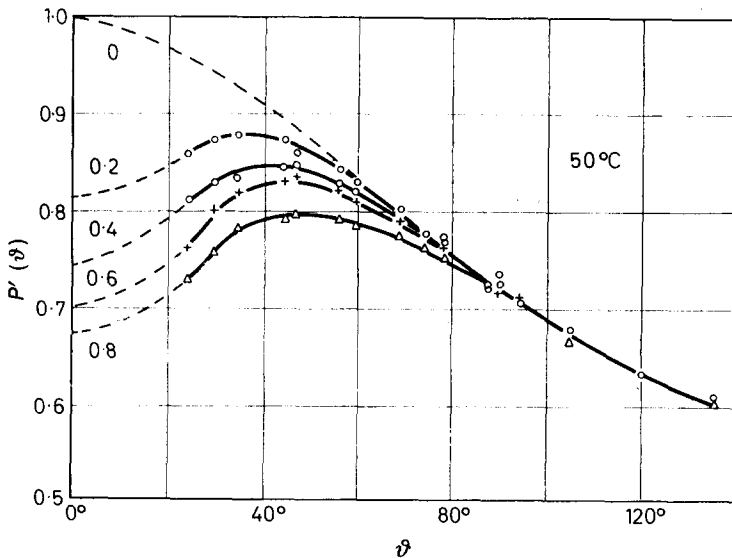


Figure 3—Plot of the apparent shape factor $P'(\vartheta) = R(\vartheta) M_w / c$ against the scattering angle ϑ

extreme case is the crystal, the high order of which causes the well known Bragg reflections. In pure fluids also the state of order is high, and therefore several scattering maxima at distinct angles appear, which are typical for the interparticle scattering¹⁰. These scattering maxima are superimposed on the shape factor of the individual particle, defined by the internal interferences. In highly diluted systems, like gases or dilute solutions, the interparticle scattering normally becomes very weak. Now the true shape factor can be determined, and the scattering intensity is almost undisturbed by other effects.

SOME THEORETICAL CONSIDERATIONS

It is easily seen that the interparticle scattering is dependent on the probability of finding a molecule at a distance r from a given molecule, and within the volume element dV . This is clearly expressed in the relationship of Zernicke and Prins¹¹.

$$P'(\vartheta) = P(\vartheta) \left[1 - 4\pi \frac{N}{V} \int_0^{\infty} (1 - g(r)) r^2 \frac{\sin sr}{sr} dr \right] \quad (3)$$

$$s = (4\pi/\lambda) \sin \vartheta/2$$

in which $P(\vartheta)$ describes the particle scattering and the second term in brackets the interparticle scattering. N is the number of molecules in the volume V , and $g(r)$ is the radial density distribution. It describes the deviations from the average probability to find from a given molecule another one within a distance r . In other words, $g(r)$ describes the order of the system, and can be calculated from the equation of Born and Green by means of statistical thermodynamics using a series expansion¹². If this series is restricted then in an approximation of second order, Fournet obtains for the apparent shape factor^{9,13}

$$P'(\vartheta) = P(\vartheta) \left[1 + 4\pi \cdot c \cdot \frac{N_A}{M} \int_0^{\infty} (1 - e^{-U(r)/kT}) r^2 \frac{\sin sr}{sr} dr \right]^{-1} \quad (4)$$

where M is the molecular weight of the scattering particle, N_A is Avogadro's number and c the concentration of the solute. $U(r)$ is the interaction potential between the particles.

Now it is possible to calculate the integral in equation (4) for some given interaction potentials. This has been done for three models, which will be given later. These calculations yield the following general form for the apparent shape factor

$$P'(\vartheta) = P(\vartheta) \left[1 + b \cdot c \cdot \frac{N_A}{M} (\bar{r}^2)^{3/2} \Phi(s, \bar{r}^2) \right]^{-1} \quad (5)$$

where b is a constant which is characteristic for the potentials used; the weaker the repulsion, the smaller is this constant. $\Phi(s)$ is a function of spherical symmetry and is similar to the shape factor of the molecules. For example, for particles like hard spheres, $\Phi^s(s)$ is the shape factor of a sphere with a diameter double that of the particle. \bar{r}^2 is the mean square radius, the meaning of which becomes clear if the sine in equation (4) is expanded

in a series. For the integral in equation (4) the following relationship is obtained

$$\int_0^{\infty} (1 - e^{-U(r)/kT}) 4\pi r^2 \frac{\sin sr}{sr} dr = V_{\text{excl.}} \left(1 - \frac{1}{6} s^2 \bar{r}^2 + \dots \right) \quad (6)$$

with

$$V_{\text{excl.}} = \int_0^{\infty} (1 - e^{-U(r)/kT}) 4\pi r^2 dr \quad (6')$$

and

$$\bar{r}^2 = \frac{\int_0^{\infty} (1 - e^{-U(r)/kT}) r^2 \cdot 4\pi r^2 dr}{\int_0^{\infty} (1 - e^{-U(r)/kT}) 4\pi r^2 dr} \quad (6'')$$

Equation (6') is built up in the same way as the cluster integral in the theory of the second virial coefficient, where it is called the excluded volume¹⁴. This value $V_{\text{excl.}}$ therefore may be considered as an excluded volume of the whole macromolecule, and \bar{r}^2 is the mean square radius of the excluded volume of the molecule. With this mean square radius constant b is defined thus

$$V_{\text{excl.}} = b \times (\bar{r}^2)^{3/2} \quad (6''')$$

Its value is dependent on the interaction potential $U(r)$.

QUANTITATIVE EVALUATION OF MEASUREMENTS

Guinier and Fournet have shown that the shape factor of spherical particles follows approximately a simple Gaussian curve over a broad range of

$$P(\vartheta)_{\text{sphere}} \simeq \exp \left\{ \frac{16\pi^2}{3} \frac{\langle S^2 \rangle}{\lambda^2} \sin^2 \vartheta / 2 \right\} \quad (7)$$

where $\langle S^2 \rangle$ is the mean square radius of gyration of the sphere.

From the similarity of the function $\Phi(s)$ with the shape factor of a spherical particle and from the expansion series of equation (6), it is expected that a plot of $\log \Phi = \log (P(\vartheta)/P'(0) - 1)$ against $\sin^2 \vartheta / 2$ (Guinier plot) should yield a curve with a linear initial part, the slope of which is

$$\tan \alpha = 2.303 \frac{16\pi^2}{6} \frac{\bar{r}^2}{\lambda^2} \quad (8)$$

Figure 4 demonstrates such a Guinier plot. The well defined linear initial part enables \bar{r}^2 to be determined reliably. Figure 5 shows the dependence of these radii on concentration and temperature. As can be seen $(\bar{r}^2)^{1/2}$ increases with decreasing concentration and tends to a limiting value for infinite dilution. This behaviour is quite comprehensible if a weak repulsion potential is assumed.

The increase of $(\bar{r}^2)_{c=0}^{1/2}$ with rising temperature is probably a consequence of coil expansion at elevated temperatures.

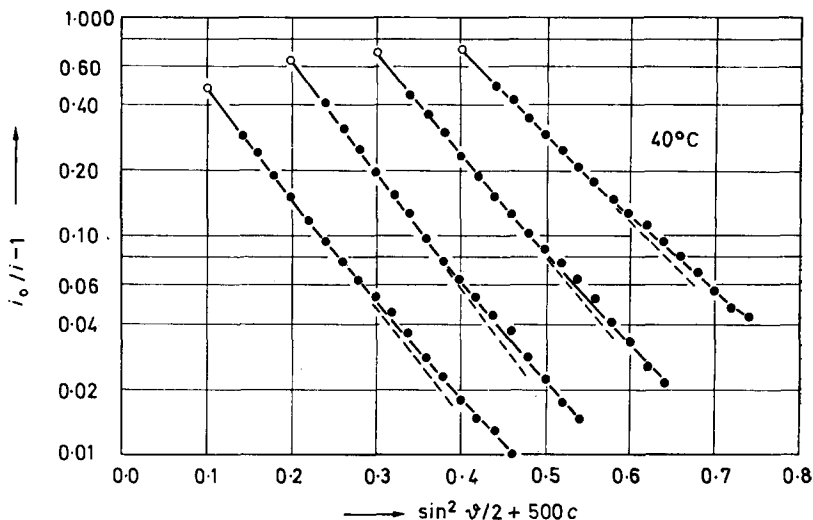


Figure 4—Plot of $\log(i_0/i - 1)$ versus $\sin^2 \theta/2 + kc$ (Guinier plot). i is the measured scattering intensity in arbitrary units and i_0 is the scattering intensity due to the straight lines in the Zimm plots of Figure 1. ($i_0/i - 1$) equals Φ in equation (5)

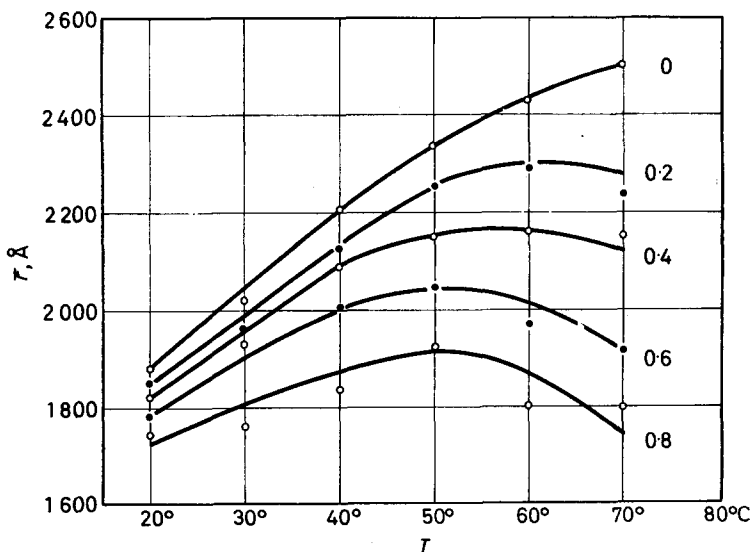


Figure 5—Dependence of r.m.s. radius of excluded volume on temperature and concentration. Numerals to the right of the curves indicate the concentrations of the polymer in g/l.

In Table 1 the radii of gyration of the molecules and the corresponding radii of the excluded volumes are compared. The latter are about six times greater than those of the coils. In other words, the coils behave approximately like spherical particles with radii that are three times those of the radii of gyration of the molecules.

INFLUENCE OF ORDER OF SOLUTIONS OF POLYVINYL CARBANILATE

Table 1. Comparison of radii of gyration of the coil ($\langle S^2 \rangle^{1/2}$) and of the corresponding excluded volume ($(\bar{r}^2)^{1/2}$)

$T, ^\circ\text{C}$	$\langle S^2 \rangle^{1/2}$	$(\bar{r}^2)^{1/2}$	$(\bar{r}^2/S^2)^{1/2}$
20	273	1 880	6.90
30	287	2 040	7.10
40	318	2 210	6.95
50	367	2 340	6.38
60	389	2 430	6.11
70	410	2 510	6.12

From the intercepts of the Guinier lines in *Figure 4* the constants b may be evaluated using equation (5). These constants are characteristic for the power of the repulsion potential. In *Figure 6* they are plotted against the

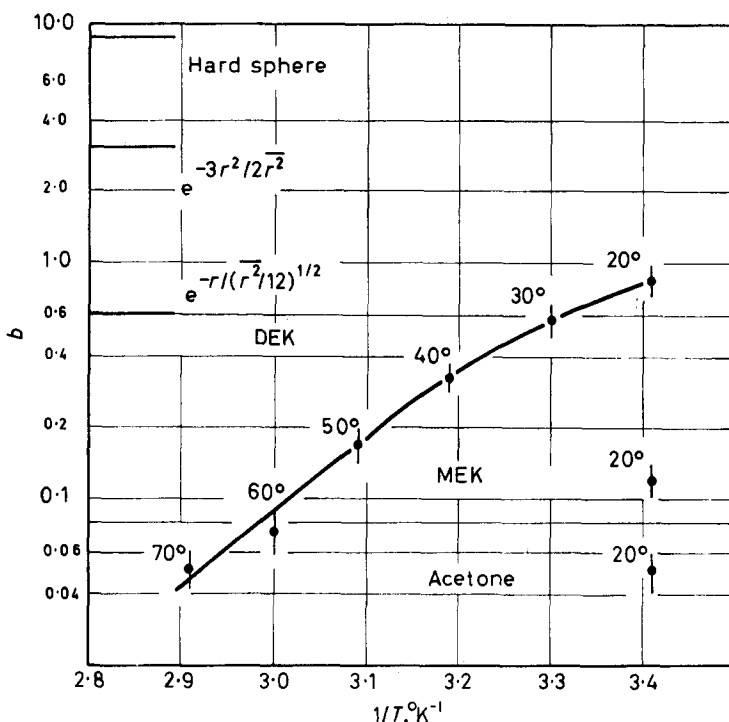


Figure 6—Plot of constant b [see equation (5)] versus the inverse temperature for solutions in DEK, MEK and acetone. The bars indicate the position of the b values of the three models mentioned in the text

reciprocal temperature. For comparison the values for the following three models have been added.

model 1: hard sphere

$$1 - e^{-U(r)/kT} = \begin{cases} 0 & \text{for } r < D \\ 1 & \text{for } r > D \end{cases}; \quad D = \left(\frac{5}{3} \bar{r}^2\right)^{1/2} \quad b = 9.05$$

model 2: highly elastic sphere (polyelectrolytes^{15,16})

$$1 - e^{-U(r)/kT} = e^{-3r^2/2\bar{r}^2}; \quad b = 3.07$$

model 3: weakly elastic sphere

$$1 - e^{-U(r)/kT} = e^{-r/(r^2/12)^{1/2}}; \quad b = 0.606$$

In solutions of DEK, b decreases with increasing temperatures. This indicates that the repulsion potential rapidly loses its efficiency with increasing temperature. Even at low temperatures the potential is weak as can be seen from the comparison of the b values of the three models mentioned above. The b values in the two other ketones are considerably smaller.

The large excluded volumes compared with the radii of gyration of the coil are not immediately understood. Thus, to make it clearer, the functions $f(r) = 1 - e^{-U(r)/kT}$ and $(\bar{r}^2)^{1/2} f(r) \cdot r^4 / \int f(r) r^2 dr$, the latter being effective for the excluded volume, have been calculated for the three models mentioned. In *Figure 7* these functions are plotted against $(r^2/\bar{r}^2)^{1/2}$. As can be seen, the hard core of the two exponential models is much smaller than that of the hard sphere. Nevertheless, the three models have the same radii of gyration for the excluded volume. This behaviour is understandable as the exponential models have long tailed potentials in contradistinction to the hard sphere model.

DISCUSSION

Similar perturbations of Zimm plots by external interferences as reported above were first observed in 1952 by Doty and Steiner¹⁵ in the case of bovine serum albumin and later on polyelectrolytes dissolved in a medium of low ionic strength¹⁶. The reason for the observed interparticle scattering is clear in these cases. As the polyelectrolytes are partly dissociated in the mentioned media, the strong electric potential of the macroions prevents an approximation below a distinct region. Therefore, the excluded volumes of the macroions are considerably higher, and this is responsible for a high order in the solution. Through addition of a suitable salt the dissociation may be suppressed, and thus the effect of interparticle scattering is made to vanish. The polyelectrolyte molecules are able to approach each other more and more and their clouds of segments partly overlap. Finally, only the excluded volume of the segments is effective. The dimensions of these segments are very small compared with the wavelength of the light, and thus the second term in the bracket of equation (5) can be neglected. Now the non-dissociated polyelectrolyte molecule corresponds to a non-polyelectrolyte coil. However, PVCarb is not a polyelectrolyte coil, and interparticle scattering should not appear. Yet the measurements in DEK indicate that the overlapping of segment clouds from different coils is hindered by a repulsion potential. This potential is not very strong, as in general the constant b in equation (5), which is typical for the potential, is smaller than that of the very weak potential of model 3.

From measurements of the intrinsic viscosities it can be concluded that an energy of activation is necessary to change a distinct state of the coil. This is recognized in the following argument.

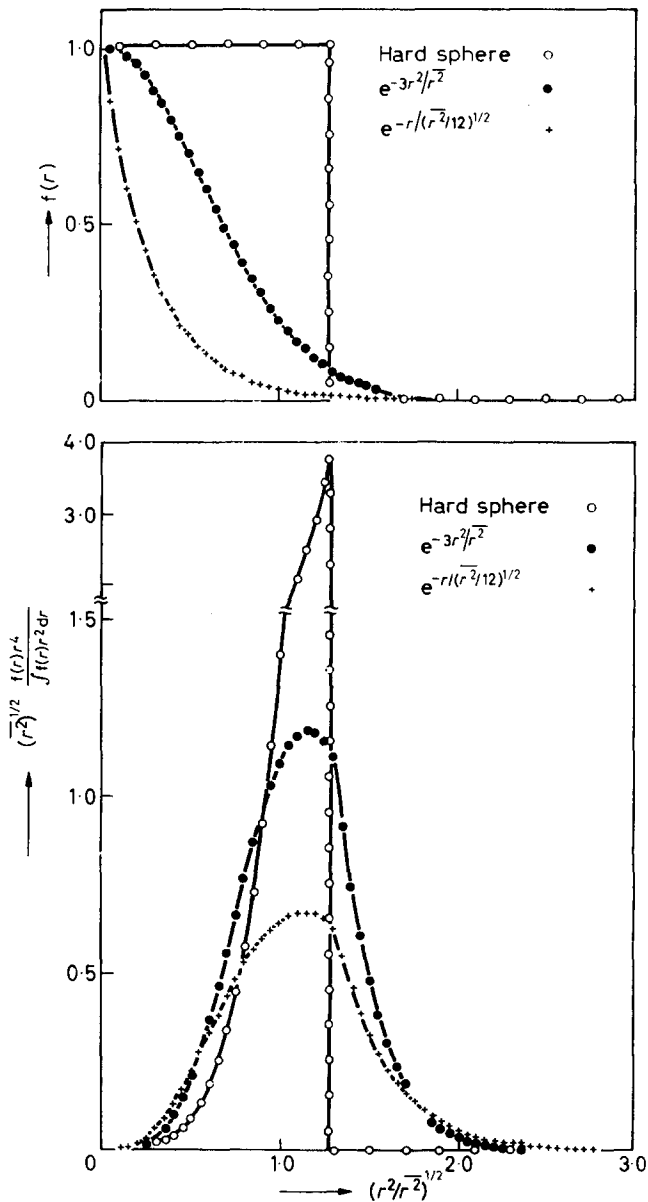


Figure 7—Dependence of the functions $f(r)=1-\exp(-U(r)/kT)$ and $(r^2/r^2)^{1/2} f(r) r^4 / \int f(r) r^2 dr$ on the reduced radius $(r^2/r^2)^{1/2}$

Taking $(\eta_{sp}/c)_\infty$ as the reduced specific viscosity for an infinitely long time after a perturbation of a coil state and $(\eta_{sp}/c)_t$ as the reduced specific viscosity for the time t , then a plot of $\log [\eta_{sp}(\infty) - \eta_{sp}(t)]/c$ against time t yields the curves of Figure 8. After a rapid initial decay, the equilibrium of the new state is reached and this is followed by a relaxation process of

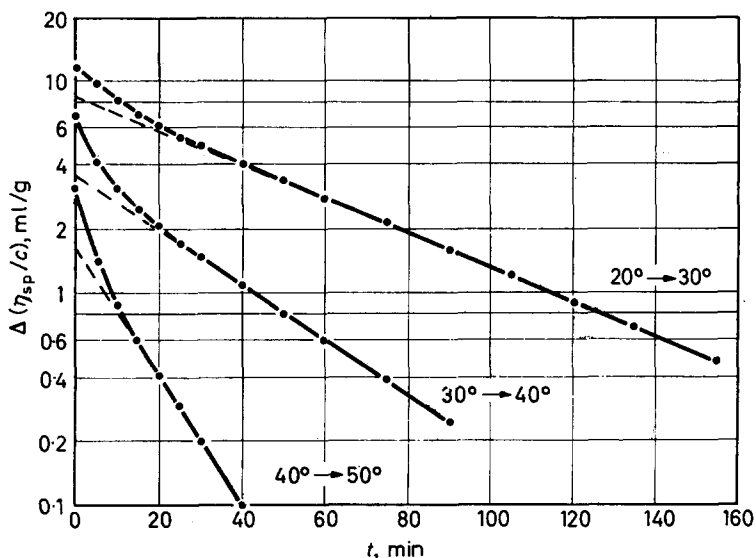


Figure 8—Plot of $\log [\eta_{sp}(\infty) - \eta_{sp}(t)]/c$ versus time for the viscosity measurements in DEK carried out after a temperature jump of 10 deg. C (cf. Figure 2)

the first order. The mean decay constant k may be determined from the slope of the asymptotic straight line. From the Arrhenius plot of these constants an average of activation of about 12 kcal per mole macromolecule is obtained.

The repulsion potential and the energy of activation could perhaps be caused by two effects, the first being that between NH and CO groups of two different substituents, hydrogen bonds may be formed. If these bonds appear only intramolecularly, i.e. only within one coil, the formerly flexible coil will now be fixed like wire netting, and this will prevent overlapping of the segment clouds. But these H bonds may also appear at higher concentrations between the substituents belonging to different coils. Hence association phenomena and gel formation at very high concentrations should appear. These effects were not observed. The second possibility is that a strong solvation due to H bonds between CO groups of the ketone and NH groups of the polymer could occur, with the effect that the solvent molecules become immobilized within the coil. Such a coil will also resist.

According to the experiments reported here it remains undecided which of the two possibilities is more realistic, yet there are some other observations that indicate the second interpretation to be true. In DEK at 35°C, i.e. a Θ -temperature, PVCarb behaves hydrodynamically like an undrained coil, while in other solvents the coil seems to be partly drained. Furthermore, the formerly undrained coil at low temperatures becomes more and more drained as the temperature is raised^{5,8}. This is in agreement with the light scattering measurements, where the repulsion potential loses efficiency with increasing temperatures.

I wish to thank Miss G. Becker for her kind assistance with light scattering measurements. I am also indebted to the Deutsche Forschungsgemeinschaft for its support.

*Institut für makromolekulare Chemie der Universität,
Freiburg i. Br., Germany*

(Received November 1967)

REFERENCES

- ¹ ZIMM, B. H. *J. chem. Phys.* 1948, **16**, 1093
- ² INAGAKI, H. and MATSUO, T. *Makromol. Chem.* 1963, **53**, 130
- ³ HUSEMANN, E., PFANNEMÜLLER, B. and BURCHARD, W. *Makromol. Chem.* 1963, **59**, 1
- ⁴ KRATOCHVIL, J. *Coll. Czech. Chem. Commun.* 1964, **29**, 2763
- ⁵ BURCHARD, W. *Z. phys. Chem., N.F.* 1964, **43**, 265
- ⁶ UTIYAMA, H. and KURATA, M. *Bull. Inst. Chem. Res., Kyoto Univ.* 1964, **42**, 128
- ⁷ UTIYAMA, H. *J. phys. Chem.* 1965, **69**, 4138
- ⁸ BURCHARD, W. and NOSSEIR, M. *Makromol. Chem.* 1965, **82**, 109
- ⁹ GUINIER, A. and FOURNET, G. *Small-Angle Scattering of X-Rays*. Wiley: New York and London, 1955
- ¹⁰ KRUIJ, R. F. *Chem. Rev.* 1962, **62**, 319
- ¹¹ ZERNICKE, F. and PRINS, J. A. *Z. Phys.* 1927, **41**, 184
- ¹² BORN, M. and GREEN, M. *Proc. Roy. Soc. A*, 1946, **188**, 10; 1947, **189**, 103
- ¹³ FOURNET, G. *C.R. Acad. Sci., Paris*, 1949, **228**, 1421
- ¹⁴ MCMILLAN, W. G. and MAYER, J. E. *J. chem. Phys.* 1945, **13**, 276
- ¹⁵ DOTY, P. and STEINER, F. *J. chem. Phys.* 1952, **20**, 85
- ¹⁶ OTH, A. and DOTY, P. *J. phys. Chem.* 1952, **56**, 43